

Radio propagation in non-uniform media

Dieder Van den Broeck,^{a,*} Stijn Buitink,^a Krijn de Vries,^a Tim Huege^{a,b} and Uzair Latif^a

^a*IIHE, Vrije Universiteit Brussel, Brussel, Belgium*

^b*Institute for Astroparticle Physics (IAP), Karlsruhe Institute of Technology, Karlsruhe, Germany*

E-mail: Dieder.jan.van.den.broeck@vub.be, Stijn.Buitink@vub.be

It has been established that, in naturally occurring ice, exotic propagation modes exist for radio signals. An interesting consequence of this is that it seems possible for signals to propagate to the receiver from an area which lies in the expected shadow zone. We present a ray tracing script based on Fermat's principle that has been developed with the aim to model and understand these propagation modes. The results of this script have been found in agreement with an earlier prediction that over-densities are able to guide the ray paths. In addition to the in-ice problem of propagation modes we use this approach to evaluate approximations made in air-shower radio emission simulations and verify if the approximations break down for certain geometries.

*9th International Workshop on Acoustic and Radio EeV Neutrino Detection Activities - ARENA2022
7-10 June 2022
Santiago de Compostela, Spain*

*Speaker

1. Introduction and motivation

The polar ice has proven to be an interesting detection medium for astroparticle physics experiments. While the deep-ice is considered pure and uniform, a gradient in density and optical properties exists close to the surface. On top of this gradient it has been indicated in [1] that perturbations exist in the ice that could cause observed exotic RF propagation modes. The understanding of these perturbations and the signal propagation in non uniform media is crucial for the design of next-generation neutrino radio detectors [2, 3, 4].

Signal propagation can be studied by using different available simulation methods. A precise but also computationally expensive option is to make use of Finite Difference Time Domain (FDTD) methods. Alternatively, one could make use of a parabolic equation solver as described in [5]. The currently most prominent method is to use raytracing, in which the signal propagation is treated as a problem in geometrical optics. The advantage is that it can be faster than the above mentioned alternatives. The disadvantage is that the analytical raytracers currently in use rely on a smooth exponential model for the index of refraction in ice. To introduce perturbations, typically one has to move to less computationally efficient numerical ray tracers. It is also noteworthy that the geometrical optics approach is expected to be valid only when wavelengths are small compared to the scale of variations in the medium.

Described in the rest of this writing is the description and results of a raytracing script based on Fermat's principle that has been developed to look into the propagation of radio signals in non-uniform media.

2. Raytracing and Fermat's principle

The derivation of a raypath can be done by starting from Fermat's principle, which postulates that light travels along paths for which the travel time is stationary [6]. To quantify this, one can introduce the concept of optical path length (OPL):

$$\text{OPL} = \int_A^B n(\mathbf{r}(s)) \cdot ds \quad (1)$$

with \mathbf{r} as the expression of the path and the increment in arc length ds defined in a way such that $ds^2 = d\mathbf{r}(s) \cdot d\mathbf{r}(s)$ and that $|\frac{d\mathbf{r}}{ds}| = \dot{\mathbf{r}} = 1$ [6].

Applying variational calculus leads to the following equation:

$$\frac{\partial n}{\partial \mathbf{r}} - \frac{d}{ds} (n(\mathbf{r}(s))\dot{\mathbf{r}}) = 0. \quad (2)$$

Equation 2 is commonly referred to as the eikonal equation. It serves as a powerful tool in optics, as will be demonstrated in the next section.

2.1 Applying the eikonal equation in 2 dimensions

Assume the rays to be bounded to a plane. The general expression for the ray path \mathbf{r} is then:

$$\mathbf{r}(s) = x(s) \cdot \hat{\mathbf{x}} + z(s) \cdot \hat{\mathbf{z}}, \quad (3)$$

with \hat{x} , \hat{z} the unit vector in the x direction and z direction respectively.

The derivatives become:

$$\frac{\partial n}{\partial \mathbf{r}} = \frac{\partial n}{\partial x} \hat{x} + \frac{\partial n}{\partial z} \hat{z}, \quad (4)$$

$$\dot{\mathbf{r}} = \frac{dx}{ds} \hat{x} + \frac{dz}{ds} \hat{z}. \quad (5)$$

This turns the eikonal equation into a set of equations, one for each coordinate:

$$\frac{d}{ds} (n(x, z) \dot{x}) = \frac{\partial n}{\partial x}, \quad (6)$$

$$\frac{d}{ds} (n(x, z) \dot{z}) = \frac{\partial n}{\partial z}. \quad (7)$$

This can be simplified even further by introducing the optical momenta $p_x = n \cdot \dot{x}$, $p_z = n \cdot \dot{z}$. The two differential equations are then rewritten as a set of 4 differential equations [7]:

$$\dot{x} = \frac{p_x}{n(x, z)}, \quad (8)$$

$$\dot{z} = \frac{p_z}{n(x, z)}, \quad (9)$$

$$\dot{p}_x = \frac{\partial n}{\partial x}, \quad (10)$$

$$\dot{p}_z = \frac{\partial n}{\partial z}. \quad (11)$$

Given a set of initial conditions and a differentiable expression for the index of refraction profile, this set of differential equations can be solved numerically to find the ray path bound in the xz plane.

3. Modelling the index of refraction

3.1 In-ice

Naturally occurring ice sheets have a density gradient in the upper layers due to compression under gravity. This leads to a structure called the firn: relatively loosely packed snow at the surface and solid ice further down.

This density gradient can be linked to an index of refraction gradient. Following the previous gravitational argument one can find an exponentially governed index of refraction profile depending on depth [1]:

$$n(z) = n_{\text{ice}} - \Delta n \cdot e^{z/z_0}. \quad (12)$$

With $z = 0$ representing the surface and z negative when going into the ice. The Δn parameter gives the difference between the refractive index at the top n_{snow} and the asymptotic value n_{ice} . The parameter z_0 represents how fast the transition takes place. While this exponential profile is a good baseline, previous measurements have also found perturbations [8].

These perturbations are crucial when describing the in-ice propagation modes. As was shown

in [1], these perturbations could form a slab waveguide and trap the rays. The formalism described above allows one to perform ray tracing with perturbations added to the index of refraction profile. To include the perturbations a differentiable function can be added to the exponential index of refraction profile.

3.2 In-Air

The ray tracer also can be used to study in-air geometries. For our purposes we can assume a simple static atmosphere model where the index of refraction depends only on height:

$$n(z) = A + B \cdot e^{-C \cdot z}.$$

The atmosphere can be modelled using different physical layers where one works with different values for A , B and C depending on the value of z . Examples of such atmosphere models can be found in the CORSIKA user manual [9] where the profiles are defined as being mass overburden profiles. These mass overburden profiles can then be translated to density and index of refraction profiles.

4. The boost factor

4.1 Cerenkov radiation in uniform media

To describe geometric boosting, we introduce the boost factor:

$$\left(\frac{dt}{dt'} \right)^{-1}$$

with t the observer time and t' the emission time. When the boost factor is large, signals emitted at different t' values arrive at nearly the same time t at the observer. This burst, which is simply due to geometry, is at the core of what is often described as Cerenkov radiation.

To see this relation more clearly consider the geometry of figure 1 where the temporal origin is taken at the impact point of a vertical air-shower, the index of refraction is taken to be uniform and the emitter travels at velocity $v = \beta \cdot c$, with $\beta = \frac{v}{c}$. The relation between arrival and emission times are then:

$$t = t' + \frac{n}{c} \sqrt{(-\beta c t')^2 + d^2}.$$

Taking the derivative with respect to t' gives:

$$\begin{aligned} \frac{dt}{dt'} &= 1 + \frac{n}{c} \frac{1}{2R} \cdot 2\beta^2 c^2 t', \\ \frac{dt}{dt'} &= 1 - n\beta \frac{z}{R}, \\ \frac{dt}{dt'} &= 1 - n\beta \cos(\theta). \end{aligned}$$

When $\frac{dt}{dt'} = 0$ it follows that $\cos(\theta) = \frac{1}{\beta \cdot n}$, which is the expression for the Cerenkov angle. The interpretation of the derivative is intuitive: when the value becomes small, signal that was emitted over an interval $\Delta t'$ arrives in a much shorter time interval Δt . An advantage of thinking in terms of $\frac{dt}{dt'}$ is that this formulation can also be used when working with non-uniform media. For the rest of this writing $\beta = 1$ shall be assumed.

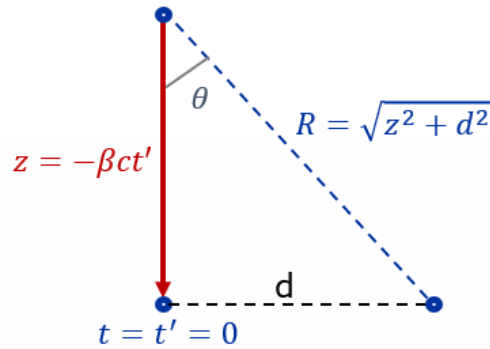


Figure 1: Geometry of a vertical airshower with values highlighted. The red arrow represents the shower axis and the point of impact is taken as the point where $t = 0$.

4.2 Generalisation to non-uniform media

It is useful to look for a generalisation of the uniform media relation $\frac{dt}{dr} = 1 - n \cdot \cos(\theta)$ for non uniform media, since this directly ties in to how the electric field is computed in Monte Carlo codes such as the end point formalism.

An immediate question is what value to use for n and θ . For a path $\mathbf{r}(s)$ between points A and B, such as shown in figure 2, there are multiple options to explore. For the index of refraction

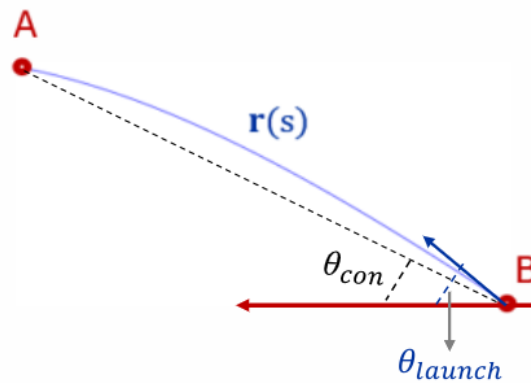


Figure 2: A raypath with different angles highlighted. The red arrow represents a simple line model for a cascade.

one could take: n at A, n at B or n averaged along $\mathbf{r}(s)$. For the value of θ one could use the angle of the straight line connecting points A and B, θ_{con} , or use the initial launch angle of the ray θ_{launch} . The current standard for in air geometries is to take θ_{con} and n at the emission point. From the raytracing script it is found that over a wide range of atmospheric geometries, the estimator that uses n at the emission point and the launch angle closely follows the numerically estimated boost factor. An example of this comparison can be found in figure 3. The geometry used for these plots is shown in figure 4. One can see that the difference between the different estimators matters more for highly inclined showers, while the straight line approximation seems to hold for the less

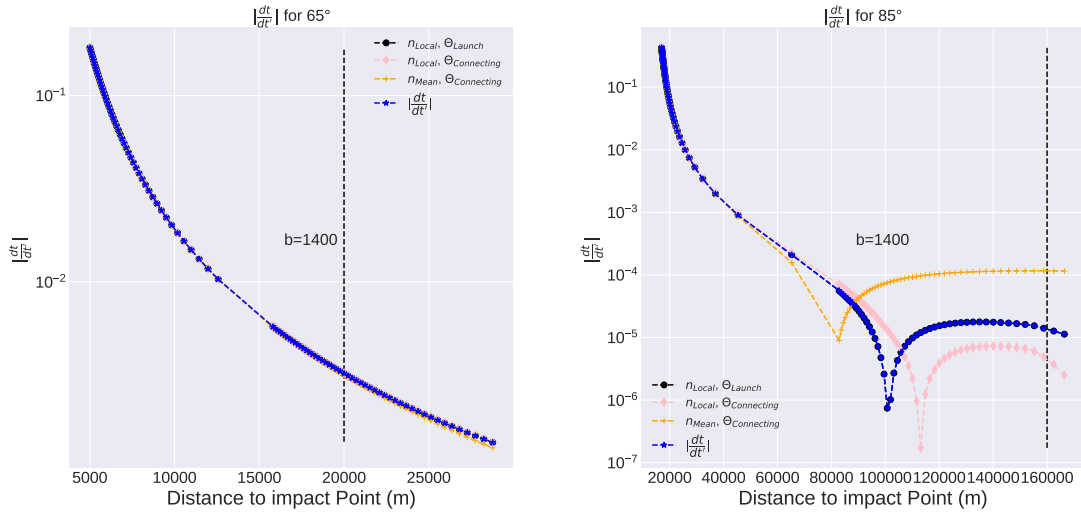


Figure 3: The numerically computed derivative compared to different values for $1 - n \cos \theta$. Left: The comparison for a geometry with impact parameter 1400 m and a zenith angle of 65° , Right: The comparison for impact parameter 1400 m and zenith angle 85° . The x axis represents the distance D along the cascade. The dotted black line represents a region from which to expect signal.

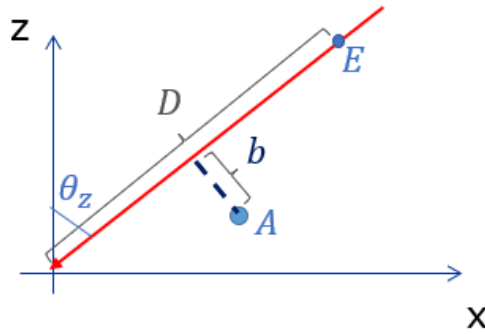


Figure 4: Geometry and values used for the raytracing script. A cascade propagates along a line defined by a zenith angle θ_z and an impact parameter b distance from receiver point A . D represents the distance between an emission point E and the point where the shower hits the ground.

inclined geometry. In other words, one can expect the currently in use approximations to hold for all but the most inclined geometries. For the very inclined geometries a better approximation is to use the initial launch angle of the ray instead of the straight line connecting angle between emitter and receiver.

5. Perturbations in ice

Following the predictions from [1] the raytracing script can also be used to investigate rays being trapped inside a perturbation in ice. The results of an in-ice geometry simulation is shown in

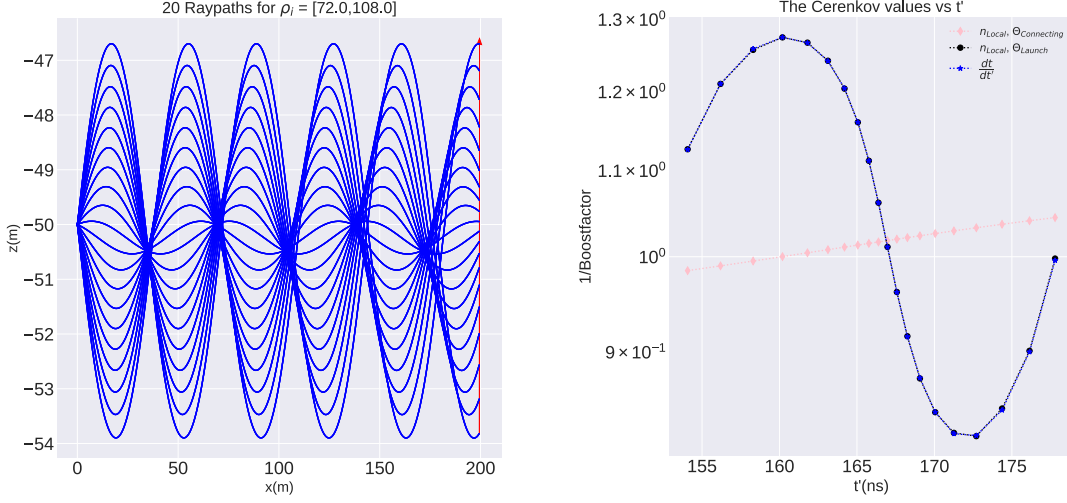


Figure 5: Left: In ice raypaths computed within an overdensity, with the red arrow denoting the line model for the cascade. Right: Cerenkov estimators and numerically computed derivative.

figure 5, where the starting point for the rays is placed within an over-density at $z = -50 \text{ m}$. The raytracer confirms that rays can stay trapped inside this overdensity which is modelled as a cosine on top of the exponential gradient:

$$n(z) = n_{ice} - \Delta n \cdot e^{z/z_0} + 0.15 \cdot \cos(\omega_p \cdot (|z_d - z|)) \quad \forall z \in [-50 \text{ m} - R, -50 \text{ m} + R],$$

$$n(z) = n_{ice} - \Delta n \cdot e^{z/z_0} \quad \forall z \notin [-50 \text{ m} - R, -50 \text{ m} + R],$$

$$\omega_p = \frac{\pi}{2 \cdot R},$$

with $R = 5 \text{ m}$ the extent of the perturbation taken here and $z_d = -50 \text{ m}$ the depth at which the perturbation reaches peak value.

Linking this back to the boost factor, the raytracing script can also check if the approximation using n at the emission point and the launch angle still correctly describes the derivative for these extreme geometries. Also shown in figure 5 are the different values for $1 - n \cos \theta$ and the numerically computed derivative. One can see that the relation $\frac{dt}{dt'} = 1 - n_{local} \cos(\theta_{launch})$ also holds for this extreme geometry. This is a non trivial result that can be used to improve approximations within current state of the art radio emission simulations.

6. Conclusion and outlook

The raytracing script based on Fermat's principle has shown that a local region of excess in the index of refraction profile can lead to waveguide like behaviour. Furthermore it has been demonstrated that $1 - n \cdot \cos \theta_{launch}$ with n at the emission point and θ_{launch} the initial launch angle of the ray closely matches the numerically calculated $\frac{dt}{dt'}$ for both in-air and in-ice geometries. Currently these results are being taken into account for the improvement of existing analytical raytracers and for the study of radiation coming from a shower core travelling from air into ice [10][11].

References

- [1] S.W. Barwick et al. “Observation of classically ‘forbidden’ electromagnetic wave propagation and implications for neutrino detection.” In: *Journal of Cosmology and Astroparticle Physics* 2018.07 (July 2018), pp. 055–055. ISSN: 1475-7516. DOI: 10.1088/1475-7516/2018/07/055. URL: <http://dx.doi.org/10.1088/1475-7516/2018/07/055>.
- [2] J. A. Aguilar et al. *The Next-Generation Radio Neutrino Observatory – Multi-Messenger Neutrino Astrophysics at Extreme Energies*. 2019. DOI: 10.48550/ARXIV.1907.12526. URL: <https://arxiv.org/abs/1907.12526>.
- [3] Jaime Álvarez-Muñiz et al. “The Giant Radio Array for Neutrino Detection (GRAND): Science and design”. In: *Science China Physics, Mechanics & Astronomy* 63.1 (Aug. 2019). DOI: 10.1007/s11433-018-9385-7. URL: <https://doi.org/10.1007/2Fs11433-018-9385-7>.
- [4] P. Allison et al. “Design and initial performance of the Askaryan Radio Array prototype EeV neutrino detector at the South Pole”. In: *Astroparticle Physics* 35.7 (2012), pp. 457–477. ISSN: 0927-6505. DOI: <https://doi.org/10.1016/j.astropartphys.2011.11.010>. URL: <https://www.sciencedirect.com/science/article/pii/S092765051100209X>.
- [5] S. Prohira et al. “Modeling in-ice radio propagation with parabolic equation methods”. In: *Physical Review D* 103.10 (May 2021). DOI: 10.1103/physrevd.103.103007. URL: <https://doi.org/10.1103/physrevd.103.103007>.
- [6] Darryl D Holm. *Geometric mechanics: Dynamics and symmetry*. Vol. 1. Imperial College Press, 2008.
- [7] D. D. Holte. *Galileo unbound: the iconic eikonal equation*. https://galileo-unbound.blog/2019/05/30/the-iconic-eikonal-and-the-optical-path/?fbclid=IwAR3OuPX1U6r4kRODJGKnofJJeqgktdQyEv_8qUyNu0IqBh6_ztWDDpyRA5U.
- [8] Ilya Kravchenko, David Besson, and Josh Meyers. “In situ index-of-refraction measurements of the South Polar firn with the RICE detector”. In: *Journal of Glaciology* 50.171 (2004), pp. 522–532.
- [9] Dieter Heck et al. “CORSIKA: A Monte Carlo code to simulate extensive air showers”. In: *Report fzka* 6019.11 (1998).
- [10] Simon De Kockere et al. “Simulation of the propagation of cosmic ray air shower cores in ice”. In: *9th International Workshop on Acoustic and Radio EeV Neutrino Detection Activities — PoS(ARENA2022)015*. Vol. 424. 2022.
- [11] Uzair Latif et al. “Propagating Air Shower Radio Signals to In-ice Antennas”. In: *9th International Workshop on Acoustic and Radio EeV Neutrino Detection Activities — PoS(ARENA2022)016*. Vol. 424. 2022.